Synthesis of Dendrimer-Passivated Noble Metal Nanoparticles in a Polar Medium: Comparison of Size between Silver and Gold Particles

Abhijit Manna,[†] Toyoko Imae,*[,†] Keigo Aoi,[‡] Masahiko Okada,[‡] and Toshinobu Yogo[§]

Research Center for Materials Science, Nagoya University, Nagoya 464-8602, Japan, Graduate School of Bioagricultural Sciences, Nagoya University, Nagoya 464-8601, Japan, and Graduate School of Engineering, Nagoya University, Nagoya 464-8603, Japan

Received May 23, 2000. Revised Manuscript Received February 21, 2001

The synthesis of silver and gold metal nanospherical particles stabilized by the fourth-generation poly(amido amine) (G4 PAMAM) dendrimer is reported. The reduction of silver nitrate and sodium tetrachloroaurate in the presence of the PAMAM dendrimer having terminal amine groups results in the formation of stable, water-soluble nanoparticles. The formation and size of the particles have been determined from the UV−vis plasmon absorption band and transmission electron microscopic (TEM) analyses. The average particle sizes are (6.2 ± 1.7)−(12.2 ± 2.9) nm for silver and are (3.2 ± 0.7)−(7.3 ± 1.5) nm for gold, depending on the metal ion-to-dendrimer terminal amine ratio (M:D) used. Thus, dendrimer-protected silver particles are substantially larger than the gold particles synthesized in similar systems. Nanoparticles prepared at 0.25:1 and lower M:D ratios are stable for a long period of time. A TEM study of the morphology also shows a short-ranged hexagonal arrangement of particles in a monolayer onto the carbon-coated copper TEM grid. Detailed particle size analysis studies by TEM support the possibility that the terminal amino groups of the dendrimers take part in the stabilization of the nanoparticles. The evidence from X-ray photoelectron spectroscopic and Fourier transform infrared absorption spectroscopic investigations confirms the valence state of the gold and the encapsulation by the dendrimer.

Introduction

The reduced sizes and dimensions of nanophase materials (quantum crystal) are at the basis of unique applications involving the construction of microdevices, catalysis, ultrathin films, and so forth. These potentialities are mainly due to the unusual dependence of the electronic properties on the particle size, either for metal or semiconductor particles in the nanoscale range (<100 nm). When the electrons and holes are confined within the three-dimensional potential well, the continuity of states in the conduction and valence bands is broken down into discrete states with an energy spacing, relative to the band edge, which is approximately inversely proportional to the square of the particle size.[1]

Nanoparticles have a characteristic high surface-to-volume ratio, providing sites for the efficient adsorption of the reacting substrates leading to unusual size-dependent chemical reactivity.[2] For example, colloidal Pt and Pd and bimetallic Pd@Pt and Pd@Au particles have been used as hydrogenation catalysts and Au particles catalyze the oxidation of carbon monoxide.[3] Noble metal particles have also found application in protein−colloid conjugates, where they are used as markers and tracers in optical and electron microscopy to help locate and quantitate antibody−antigen binding sites in cells and tissue.[4] The synthesis and characterization of quantum crystals have thus motivated a vast amount of work.[1−7]

* To whom correspondence should be addressed. Toyoko Imae, Research Center for Materials Science, Nagoya University, Nagoya 464-8602, Japan. E-mail: imae@chem2.chem.nagoya-u.ac.jp. Fax. + 81-52-789-5912. Tel.: + 81-52-789-5911.

[†] Research Center for Materials Science, Nagoya University.

[‡] Graduate School of Bioagricultural Sciences, Nagoya University.

[§] Graduate School of Engineering, Nagoya University.

(1) (a) Henglin, A. *Chem. Rev.* **1989**, *89*, 1861. (b) Schmid, G. *Chem. Rev.* **1992**, *92*, 1709. (c) Chakarvorty, D.; Giri, A. K. In *Chemistry of Advanced Materials*; Rao, C. N. R., Ed.; Blackwell Scientific Publication: Boca Raton, FL, 1993. (d) Schmid, G. *Clusters and Colloids*; VCH: Weinheim, 1994.

(2) (a) Hirai, H.; Wakabayashi, H.; Komiyama, M. *Bull. Chem. Soc. Jpn.* **1986**, *59*, 367. (b) Siegel, R. *Nanostruct. Mater.* **1993**, *3*, 1. (c) Boakye, E.; Radovic, L. R.; Osseo-Asare, K. *J. Collid Interface Sci.* **1994**, *163*, 120.

(3) (a) Kiwi, J.; Gratzel, M. *J. Am. Chem. Soc.* **1979**, *101*, 7214. (b) Hatuta, M.; Kobayashi, T.; Sano, H.; Yamada, N. *Chem. Lett.* **1987**, 405. (c) Vargaftik, M. N.; Zagorodnikov, U. P.; Stolarov, I. P.; Chuvilin, A. L.; Zamaraev, K. I. *J. Mol. Catal.* **1989**, *53*, 315.

(4) (a) Horrisberger, M. In *Preparation of Biological Specimens for Scanning Electron Microscopy;* Murphy, J. A., Roomans, G. M., Eds.; Scanning Electron Microscopy, Inc.: Chicago, 1984; p 315. (b) DeMey, J. *EMSA Bull.* **1984**, *14*, 54.

(5) Brust, M.; Walker, M.; Bethell, D.; Schiffrin, D. J.; Whyman, R. *J. Chem. Soc., Chem. Commun.* **1994**, 801.

(6) (a) Terrill, R. H.; Postlethwaite, T. A.; Chen, C.; Poon, C. D.; Terzis, A.; Chen, A.; Hutchison, J. E.; Clark, M. R.; Wignall, G.; Londono, D. J.; Superfine, R.; Falvo, M.; Johnson, C. S., Jr.; Samulski, T. E.; Murray, R. W. *J. Am. Chem. Soc.* **1995**, *117*, 12537. (b) Andres, R. P.; Bielefeld, J. D.; Henderson, J. I.; Janes, D. B.; Kolagunta, V. R.; Kubiak, C. P.; Mahoney. W.; Osifchin, R. F. *Science* **1996**, *273*, 1690.

(7) (a) Golden, J. H.; Deng, H.; Fréchet, J. M. J. *Science* **1995**, *268*, 1463. (b) Spatz, J. P.; Roesher, A.; Moller, M. *Adv. Mater.* **1996**, *8*, 337. (c) Carrot, G.; Valmalette, J. C.; Plummer, C. J. G.; Scholz, S. M.; Dutta, J.; Hoffmann, H.; Hilborn, J. G. *Colloid Polym. Sci.* **1998**, *276*, 853.

10.1021/cm000416b CCC: $20.00
Published on Web 04/07/2001

The control of the size and/or polydispersity of the particles is carried out using various colloidal systems such as reverse micelles, microemulsions, Langmuir−Blodgett films, organometallic techniques, and two-phase liquid−liquid systems.[5,8−11] The achievement of accurate control of the size, stability, and reactivity of the quantum particles is required to allow the attachment to the surface of substrates or other particles without leading to coalescence and hence losing their size-induced electronic properties. Moreover, the ability of particles to arrange into well-defined two- and three-dimensional spatial configurations should produce novel properties such as new collective physical behavior.[12] It is known that the manipulation of nearly monodispersed nanometer-size crystallites presents a number of difficulties. The development of a general procedure for the fabrication of quantum crystals is a major challenge for future research. The fabrication of such crystals of particles would, for example, lead to the production of optical gratings, optical filters, data storage, microelectronic devices, and selective solar absorbers.[12,13]

Highly branched dendrimer molecules with polar terminal groups, such as amino, thiol, hydroxyl, and carboxyl groups, are water-soluble and chemisorbed (i.e., formed self-assembled monolayer, SAM) onto the solid surfaces of metals or oxides derived from their molten and/or solution states.[14,15] In solution these molecules behave as unimolecular micelles (nanospheres). The combination of a catalytic core with such a micellar arrangement holds much promise for the development of organic chemistry in aqueous media and for the mimicry of biological systems. The adsorption behavior opens new ways for the preparation of well-defined molecular objects and devices, which are very useful in the development of new technology. Recently, Balogh et al.,[16] Crooks and his collaborators,[17] and Esumi et al.[18] reported the synthesis of dendrimer-stabilized gold and copper nanoparticles. However, it is not clear within the scientific community which part of the dendrimer is responsible for the stabilization of gold nanoparticles. In their initial work, Crooks and his collaborators[17a,b] postulated that nanoparticles are stabilized by the core nitrogen atoms of the dendrimer molecules. However, later they noted that terminal amino groups are extremely effective for the stabilization of gold nanoparticles.[17c] Very recently, Imae et al.[19] reported the surface interaction force between the fourth-generation poly(amido amine) (G4 PAMAM) dendrimers adsorbed onto clean glass surfaces from its aqueous solution. The results confirmed that the interaction force between dendrimer layers is dominated by the osmotic pressure effect in the steric repulsion force. This indicates that dendrimers with repulsive intermolecular interactions can be utilized as a surface-improvement agent promoting the dispersion stability of fine particles in a polar solvent medium. Thus, further detailed studies are needed to draw a conclusion about the active part of the dendrimer that is involved in the stabilization of nanoparticles.

In this study, we explored the potential of dendrimers in the passivation of silver and gold nanoparticles. Previous studies of the synthesis of dendrimer-passivated nanoparticles have been reported for the platinum, gold, and copper metals.[16−18] The microstructure and optical properties of alkanethiol-stabilized gold and silver particles adsorbed onto dendrimer-modified silicon oxide surfaces have also been reported in the literature.[20] We have synthesized G4 PAMAM dendrimer-protected silver nanoparticles at various number ratios (M:D) of metal ion to terminal primary amino group of the G4 PAMAM dendrimer and compared these with the gold systems. The particle formation and the sizes were determined from the UV−vis plasmon absorption bands and transmission electron micrographs, respectively. The valence states of the metal nanoparticles and the protection ability of the dendrimer were determined by X-ray photoelectron spectroscopic (XPS) and Fourier transform infrared (FT-IR) spectroscopic investigations, respectively.

Experimental Section

Reagents. Silver nitrate ($AgNO_3$, 99.99%), sodium tetrachloroaurate(III) dihydrate ($NaAuCl_4 \cdot 2H_2O$, 99%), and sodium borohydride ($NaBH_4$, 99%) were purchased from Aldrich Chemical Co. Methanol (MeOH) (99.8%) was purchased from Wako Chemical Co. All of these chemicals were used without modification. Milli-Q water was used throughout all experiments. G4 PAMAM dendrimer was synthesized according to the procedure in the literature.[14,20]

Synthesis of Dendrimer-Protected Ag and Au Nanoparticles. The synthesis procedure is similar to that reported in the literature.[17c] Two cubic centimeters of salt solution ($AgNO_3$ 0.75, 1.5, 2.5, 5, 10, 25, 100 mM or $Na[AuCl_4]$ 0.75, 2.5, 10, 25, 100 mM), 0.365 g of dendrimer solution (10 wt % MeOH solution), and 0.6 cm^3 of MeOH were mixed together to produce a reaction mixture. Fifteen milligrams of $NaBH_4$ was dissolved in 2 cm^3 of MeOH:water (1:2 in volume) mixture, and the entire $NaBH_4$ solution was slowly added to the reaction mixture while stirring. The reaction mixture turned to a yellow or brown color within a few seconds after addition of the first drop of the $NaBH_4$ solution. The stirring was continued for 2 h to complete the reaction. Finally, we obtained a yellow or brown colloidal solution in a MeOH:water (1:2 in volume) mixture of dendrimer-passivated nanoparticles.

(8) (a) Fendler, E. J.; Fendler, J. H. *Micelle and Macromolecular Catalysis Systems*; Academic Press: New York, 1975. (b) Fendler, J. H.; Meldrum, F. C. *Adv. Mater.* **1996**, *7*, 607.

(9) Soriage, M. P.; Hubbard, A. T. *J. Am. Chem. Soc.* **1982**, *104*, 3937.

(10) (a) Pilani, M. P. *J. Phys. Chem.* **1993**, *97*, 6961. (b) Chang, C.; Fogler, H. S. *Langmuir* **1997**, *13*, 3295.

(11) Manna, A.; Kulkarni, B. D.; Bandyopadhyay, K.; Vijayamohanan, K. *Chem. Mater.* **1997**, *9*, 3032.

(12) (a) Hamilton, J. F.; Baetzold, R. C. *Science* **1979**, *205*, 1213. (b) Heitman, D.; Kotthaus, J. P. *Phys. Today* **1993**, *56*. (c) Colvin, V. L.; Schlamp, M. C.; Alivisatos, A. P. *Nature* **1994**, *370*, 354.

(13) Brus, L. *J. Phys. Chem.* **1986**, *90*, 2555.

(14) (a) Tomalia, D. A.; Naylor, A. M.; Goddard, W. A., III *Angew. Chem., Int. Ed. Eng.* **1990**, *29*, 138, (b) Fischer, M.; Vögtle, F. *Angew. Chem., Int. Ed.* **1999**, *38*, 364.

(15) Tomalia, D. A.; Balogh, L. U.S. Patent Application, 08924790, Sep 5, 1996.

(16) (a) Balogh, L.; Swanson, D. R.; Spindler, R.; Tomalia, D. A. *Polym. Mater. Sci. Eng.* **1997**, *77*, 118, (b) Balogh, L.; Tomalia, D. A. *J. Am. Chem. Soc.* **1998**, *120*, 7355, (c) Balogh, L.; Tomalia, D. A.; Hagnauer, G. L. *Chem. Innov.* **2000**, *30*, 19.

(17) (a) Zhao, M.; Sun, L.; Crooks, R. M. *J. Am. Chem. Soc.* **1998**, *120*, 4877. (b) Zhao, M.; Crooks, R. M. *Angew. Chem., Int. Ed.* **1999**, *38*, 364. (c) Garcia, M. E.; Baker, L. A.; Crooks, R. M. *Anal. Chem.* **1999**, *71*, 256.

(18) Esumi, K.; Suzuki, A.; Aihara, N.; Usui, K.; Torigoe, K. *Langmuir* **1998**, *14*, 3157.

(19) Imae, T.; Funayama, K.; Aoi, K.; Tsutsumiuchi, K.; Okada, M.; Furusaka, M. *Langmuir* **1999**, *15*, 4076.

(20) Bar, G.; Rubin, S.; Cutts, R. W.; Taylor, T. N.; Zawodzinski, T. A., Jr. *Langmuir* **1996**, *12*, 1172.

The dendrimer-passivated nanoparticle solutions were very stable except for the 1:1 (M:D) ratio. The particles formed in a 1:1 (M:D) ratio were unstable in solution and precipitated. The precipitate was redispersible in a water−methanol mixture.

Characterization. Optical measurements were carried out at room temperature on a Shimadzu UV 2200 UV−vis spectrometer using a quartz cell (10-mm path). The spectral background absorption was subtracted by using the UV−vis spectra of the same solvent mixture.

Specimens for transmission electron microscopy (TEM) were prepared by spreading a small drop (2 μL) of a 20 times dilution (in a 1:2 in volume of water:methanol mixture) of the colloidal solutions onto standard copper grids coated with a thin amorphous Formver carbon film and letting the drop dry almost completely in air for nearly 1 h. The specimens were placed onto a grid holder. The size and morphology of the particles were observed at room temperature on a Hitachi H-800 electron microscope operating at 100 kV. The size distribution was derived from histograms. These were obtained by measuring the diameter of the particles from different parts of the specimen, and in every case nearly 400 particles were taken into account, except the case for the lowest M:D (0.01:1) ratio where 150 particles were counted. The standard deviation σ of the size distribution was calculated from the equation

$$\sigma = [\Sigma n_i (D_i - D)^2/(N - 1)]^{0.5}$$

where n_i is the number of particles having diameter D_i. D is the average diameter [$=(\Sigma n_i D_i)/N$] and N is the total number of particles.

FT-IR spectra in the region of 4000−700 cm^{-1} were recorded at room temperature on a Bio-Rad FTS 575C FT-IR instrument. We used a 10 wt % G4-PAMAM in CD_3OD solution to measure the spectra of the free dendrimer. The colloidal solution used for the analysis was a redispersion of the dry precipitate of the 1:1 (M:D) ratio in the CD_3OD:D_2O (1:2) mixture. Samples for the analysis were prepared by spreading a small drop of colloid dispersion onto a KBr pellet.

XPS signals were recorded on a JEOL JPS-9000MC spectrometer operated at a base pressure lower than 10^{-7} Pa. The different core level spectra were recorded using MgKα radiation ($h\nu = 1253.6$ eV) with an X-ray source operated at a power of 10.0 kV and a current of 10.0 mA. The spectra of the C(1s), O(1s), N(1s), and Au(4f) orbitals were recorded at an overall instrumental resolution of ≈0.9 eV. The sample used for this analysis was the dry precipitate of the 1:1 (D:M) ratio, which was washed by the MeOH:water (1:2 in volume) mixture and dried under the flow of N_2 gas.

Results and Discussion

Formation of Particles. Figures 1 and 2 in which the ratio in the bracket indicates the M:D ratio show the UV−vis absorption spectra of the dendrimer-protected silver and gold colloidal solutions, respectively. A dilute colloidal silver solution of lowest M:D ratio (0.01:1) displays a strong absorption in the ≈400-nm region (see Figure 1). This peak must arise from the surface plasmon absorption of the silver clusters. Silver and gold metals are known to have intense plasmon absorption bands in the visible region.[18,21] The electronic energy levels and optical transition in a "roughened" silver surface have been extensively studied and it was confirmed that the 4d to 5sp interband transition generally occurs at around an energy corresponding to 320 nm (i.e., 3.8 eV).[21] For dendrimer-capped silver nanoparticles, the characteristic plasmon absorption band at around 400 nm supports the formation of "quantum-dot" particles.[22]

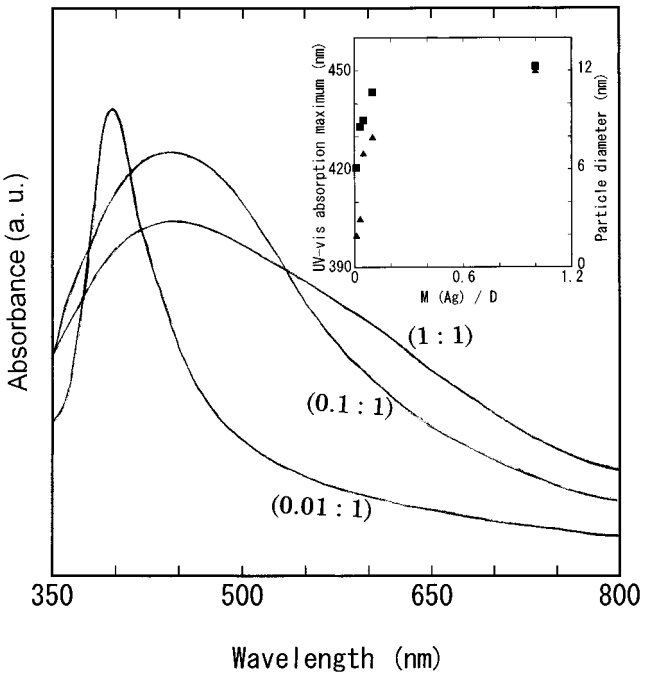

Figure 1. UV−vis spectra of silver nanoparticles coated with G4 PAMAM dendrimer in a methanol:water mixture (1:2 in volume). The ratio in every bracket indicates M:D. The insert shows the plots of the UV−vis absorption maximum (△) and particle diameter (■) vs M/D value.

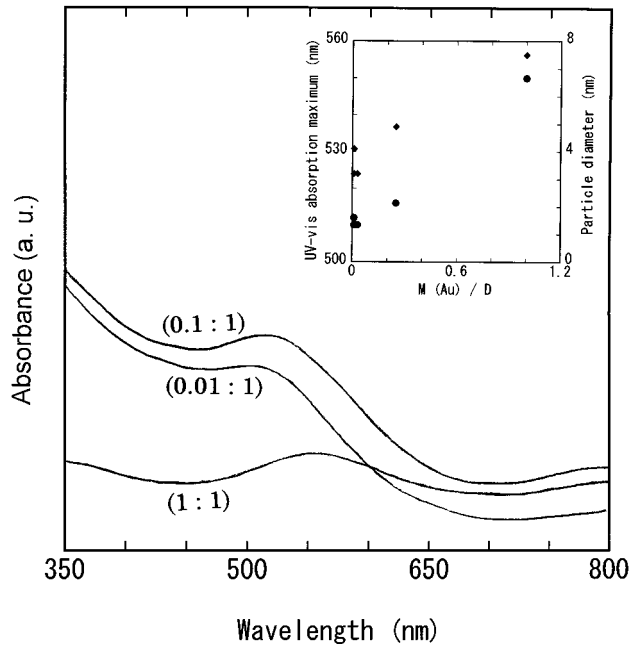

Figure 2. UV−vis spectra of gold nanoparticles coated with G4 PAMAM dendrimer in a methanol−water mixture (1:2 in volume). The ratio in every bracket indicates M:D. The insert shows the plots of the UV−vis absorption maximum (●) and particle diameter (◆) vs M/D value.

The sharpening of the spectrum obtained for the dendrimer-coated silver particles of the 0.01:1 (M:D) ratio arises because of the smaller particle size than the mean free path of the electrons (52 nm for silver). The

(21) (a) Kreibig, U. *J. Phys. F: Met. Phys.* **1974**, *4*, 999. (b) Henglein, A. *J. Phys. Chem.* **1993**, *97*, 5457.

(22) (a) Beaglehole, D.; Hunderi, O. *Phys. Rev. B* **1970**, *2*, 309. (b) Hengelin, A. *J. Phys. Chem.* **1993**, *97*, 5457.

Table 1. Characteristic Data for Dendrimer-Protected Silver Nanoparticles

concn of $AgNO_3$ solution used (mM)	Ag^+:NH_2 group (M:D) ration	λ_{max} (nm)	average particle size (diameter in nm)	standard deviation
0.75	0.01:1	400	6.2	±1.7
1.5	0.02:1	400	6.6	±1.9
2.5	0.03:1	405	8.6	±1.7
5	0.05:1	420	9.3	±2.5
10	0.1:1	425	10.8	±2.3
25	0.25:1	430	10.9	±2.8
100	1:1	450	12.2	±2.9

Table 2. Characteristic Data for Dendrimer-Protected Gold Nanoparticles

concn of $Na[AuCl_4]$ solution used (mM)	Au^{3+}:NH_2 group (M:D) ratio	λ_{max} (nm)	average particle size (diameter in nm)	standard deviation
0.75	0.01:1	510	3.2	±0.7
2.5	0.03:1	510	3.2	±0.8
10	0.1:1	512	4.0	±0.9
25	0.25:1	516	4.9	±1.3
100	1:1	550	7.3	±1.5

insert shown in Figure 1 is a plot of the M/D value versus UV−vis absorption maximum. This plot shows that when the (M/D) value (i.e., M:D ratio, used only in Figures 1 and 2 for simplicity) is changed, the peak maximum varies from 400 nm at 0.01:1 to 450 nm at 1:1 (see also Table 1). Furthermore, Figure 1 shows that the absorption maximum broadened with an increase in the M:D ratio. The red shift and broadening of the plasmon absorption peak with an increase in the M:D ratio indicate an increase in the particle size and polydispersity, respectively. This is a consequence of the limited number of dendrimer molecules available to interact with the growing particles.

Similarly, dendrimer-stabilized gold particles show plasmon absorption bands at around 500 nm, which are shown in Figure 2. The transition between the $5d^{10}$ level and unoccupied conduction bands leads the surface plasmon resonance absorption spectra for gold nanoparticles.[23] The peak maxima of the absorptions are listed in Table 2. The insert of Figure 2 shows a plot of the M:D ratio versus the UV−vis absorption maximum. This plot, Table 2, and Figure 2 show a red shift and broadening of the absorption band for higher D:M ratios, respectively, because of a similar reason for the silver particles.

Particle Size. The sizes of the particles prepared using the G4 PAMAM dendrimer at different M:D ratios were examined by TEM. The typical bright field TEM images and histograms of the size distribution are shown in Figures 3 and 4 for silver and gold particles, respectively. The images show that all the particles are almost spherical. The average size of the particles as a function of the M:D ratio used to synthesize them is given in Tables 1 and 2 for the silver and gold particles, respectively. The values of standard deviation are also included in Table 1. The average particle sizes are (6.2 ± 1.7)−(12.2 ± 2.9) nm for silver and (3.2 ± 0.7)−(7.3 ± 1.5) nm for gold, depending on the M:D ratio used. The average particle size increases with an increase in the M:D ratio, which is in agreement with our UV−vis experiments (see insert in Figures 1 and 2) and the results reported by others.[16−18]

A comparison of the particle sizes reveals that the G4 PAMAM dendrimer-protected silver particles are substantially larger than the gold particles. This size difference may be due to the following reasons. The standard redox potentials ($M^{n+} + ne \rightarrow M$) of Ag^+/Ag and Au^{3+}/Au are 0.79 and 1.002 V, respectively.[24] The lower reduction potential of the Ag^+/Ag pair favors the slower rate of reduction (compared with the Au^{3+}/Au system), resulting in the formation of larger metal particles. The other possibility for the formation of larger silver particles is the higher reactivity of the silver (Ag^0) than gold (Au^0).[25] The higher reactivity of the silver clusters favors aggregation, resulting in the formation of larger nanoparticles compared to those of the gold. The TEM micrographs also show that the dendrimer-coated particles taking part in the nanostructure formation maintain their distinct character and less aggregation into flocs, as seen in Figure 1 (0.01:1) for the silver particles and Figure 2 (0.01:1) and (0.1:1) for the gold particles.

The images in Figures 3 and 4 show that during the preparation of TEM specimens a well-defined monolayer with a hexagonal array (of nanoparticles) within a short domain was formed. The silver particles formed shorter ranged arrays in comparison with the gold particles. The best monolayer formation was obtained for the gold particles of the 0.1:1 (M:D) ratio, as seen in Figure 4. The interparticle distance measured for this system is ca. 3.3 nm. Because the ideal diameter of the G4 PAMAM dendrimer sphere is 4.5 nm,[26] this short interparticle distance can be explained on the basis of the following assumptions: (i) collapse of the dendrimer monolayer on the metal particles, similar to the structure on metal surfaces, (ii) anchorage of each dendrimer molecule to more than one particle, and (iii) formation of nanoparticles within the dendrimer interior.

As the G4 PAMAM dendrimer molecules are soft and deformable, the dendritic macromolecules within the monolayer may be highly compressed and flattened along the surface normal. Hierlemann et al.[26a] and Amis and co-workers[26b] reported that the average ellipsometric thickness and lateral dimension of an isolated G4 PAMAM dendrimer adsorbed onto naked Au surfaces are only 0.5−0.8 and 15 nm, respectively. Tsukruk et al.[27] obtained the thickness of a G4 PAMAM dendrimer monolayer adsorbed onto Si surfaces as 1.4 ± 0.3 nm, which is comparable to our results and supports our assumption (i). According to the second assumption, the diameter of a dendrimer molecule anchoring to more than one particle is nearly 3.3 nm. This assumption is also possible. In this case the dendrimer molecule is less compressed because of the polarization of the whole surface by a similar charge.[19]

(23) Alvarez, M. M.; Khoury, J. T.; Schaaff, T. G.; Shafigullin, M. N.; Vezmer, I.; Whetten, R. L. *J. Phys. Chem. B* **1997**, *101*, 3703.

(24) Emsley, J. *The Elements*, 3rd ed.; Clarendon Press: Oxford, 1998; pp 88, 192.

(25) Laibinis, P. E.; Whitesides, G. M.; Allara, D. L.; Tao, Y.-T.; Parikh, A. N.; Nuzzo, R. G. *J. Am. Chem. Soc.* **1991**, *113*, 7152.

(26) (a) Hierlemann, A.; Campbell, J. K.; Baker, L. A.; Crooks, R. M.; Ricco, A. J. *J. Am. Chem. Soc.* **1998**, *120*, 5323, (b) Grohn, F.; Bauer, B. J.; Akpalu, Y. A.; Jackson, C. L.; Amis, E. J. *Macromolecules* **2000**, *33*, 6042.

(27) Tsukruk, V.; Rinderspacher, F.; Bilznyuk, V. N. *Langmuir* **1997**, *13*, 2171.

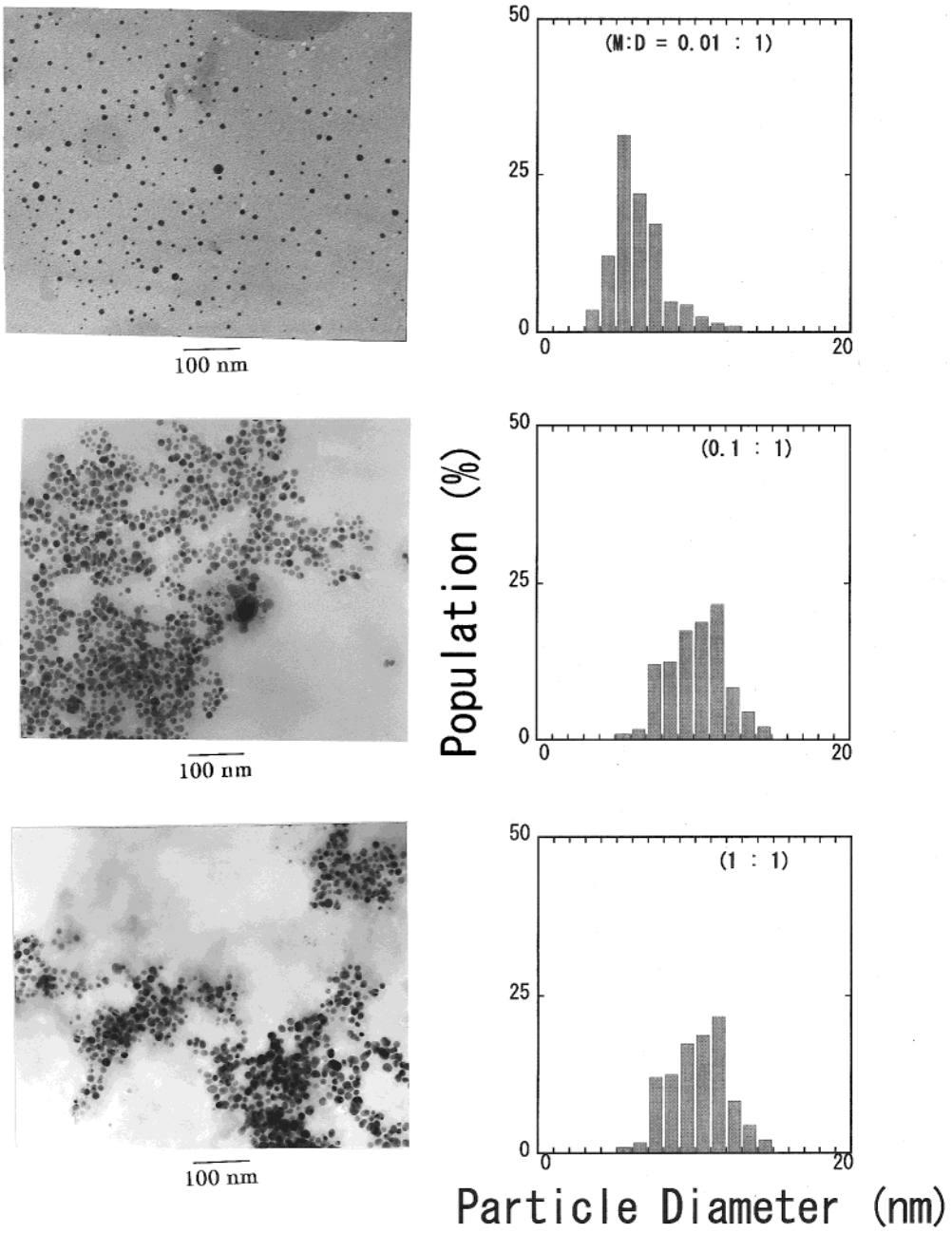

Figure 3. TEM for specimens of the G4 PAMAM dendrimer-protected silver nanoparticles. The histogram in the right-hand side of every micrograph shows the particle distribution. The ratio in every bracket indicates M:D.

According to the assumption (iii), there is also the possibility of the formation of the nanoparticles within the dendrimer interior.[16,17a,b] However, the particle size analysis shows that the minimum average sizes of the silver and gold particles are 6.2 and 3.2 nm, respectively. The particle size of the gold is comparable to previously reported results[17c] where the authors proposed the possibility of the stabilization of particles through the surface attachment of primary amino groups. The detailed studies of the silver particles in the present work show that the minimum size is 6.2 nm, which is nearly 1.5-fold larger than the hydrodynamic diameter (≈4.5 nm)[26] of the G4 PAMAM dendrimer. The core of the dendrimer is never expected to be larger than its hydrodynamic diameter. The support of assumptions (i) and (ii) evidences that the primary amino groups stabilize the nanoparticles; that is, the most active part of the dendrimer in nanoparticle stabilization is the terminal amino groups.

It is also noted that during the evaluation of our manuscript Amis and co-workers[26b] published the topology (chemistry of the stabilization) of G2-G10 PAMAM dendrimers in nanocomposite formation. They found gold particles of ≈3 nm for G10, 1.8−4 nm for G4−G9 (diameter increases with increasing dendrimer generation), and 4 nm for the G2 PAMAM dendrimer. In addition, they observed the existence of 7-nm particles for the G4 PAMAM dendrimer system (M:D = 1:1), which is comparable to our results obtained in a similar system (see Table 2). They concluded that 7-nm particles were forming because of the aggregation of dendrimers containing very small metal particles. They used different solution techniques to interpret their results. Finally, they concluded the following: (1) the formation

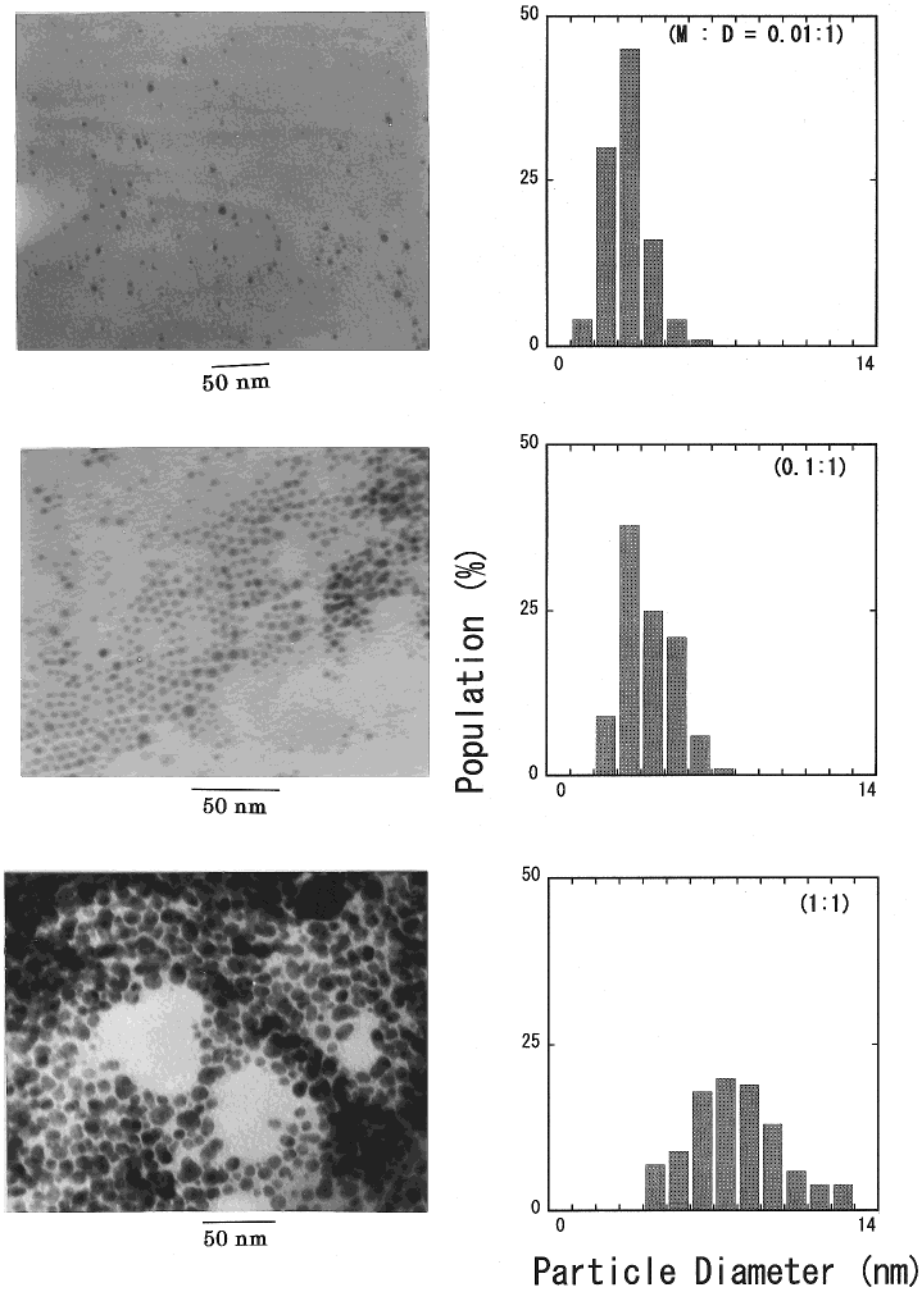

Figure 4. TEM for specimens of the G4 PAMAM dendrimer-protected gold nanoparticles. The histogram in the right-hand side of every micrograph shows the particle distribution. The ratio in every bracket indicates M:D.

of multiple smaller particles inside one dendrimer is due to a more crowded volume (insufficient chain flexibility). (2) The mid-generations (G6−G9 PAMAM dendrimers) are effective candidates to stabilize one gold particle per dendrimer molecule. (3) For the G2-G4 PAMAM dendrimer, a single molecule could not provide enough material to stabilize the surface of a single gold colloid. These dendrimers behave like lower molecular mass stabilizers and several dendrimers surround the surface of the metal particle, as we have also concluded.

Defects during monolayer formation were observed in the TEM images (Figures 3 and 4) for high M:D ratios (>0.1:1). This can be attributed to the poor wetting properties of the solvent (1:2 MeOH:water mixture) to the hydrophobic surfaces. Similar defects were observed for a monolayer of long-chain alkanethiol-coated silver nanoparticles of average size <5 nm but not for the bigger particles (>5 nm).[28] In our cases, we observed the formation of defects even for particle sizes larger than 10 nm.

The formation of a long-ranged particle monolayer is very rare in the case of low M:D (0.01:1) ratios due to the low particle concentrations.

Particle Encapsulation and the Oxidation States of the Metal. Figure 5 shows a comparison of the FT-IR spectra between 4000 and 700 cm^{-1} of the free dendrimer and encapsulated particles, where the characteristic bands of the G4 PAMAM dendrimer are clearly seen.[29] The band positions and their assignments are listed in Table 3. The similarity of the features of

(28) (a) Ohara, P. C.; Heath, J. R.; Gelbart, W. M. *Angew. Chem., Int. Ed. Eng.* **1997**, *36*, 1077. (b) Motte, L.; Pilani, P. *J. Phys. Chem. B* **1998**, *102*, 4104.

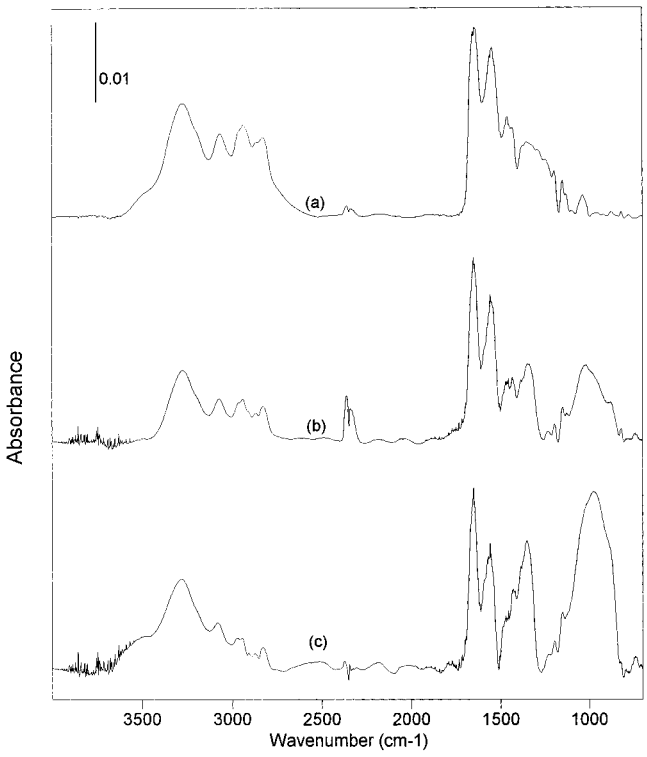

Figure 5. FT-IR spectra of (a) G4 PAMAM dendrimer and (b) dendrimer-protected silver nanoparticles and (c) dendrimer-protected gold nanoparticles.

Table 3. FT-IR Bands for a Dendrimer and Dendrimer-Coated Nanoparticles

	band position[a]		
assignment	free dendrimer	silver nanoparticle	gold nanoparticle
amide A	3272 (s)	3276 (s)	3279 (s)
amide B	3068 (m)	3072 (m)	3080 (m)
	2969 (sh)	2971 (sh)	2976 (m)
CH_2 antisymmetric stretching	2943 (m)	2944 (m)	2945 (m)
	2907 (sh)	2908 (w)	2909 (w)
	2868 (w)	2874 (w)	2879 (w)
CH_2 symmetric stretching	2830 (m)	2830 (m)	2831 (m)
amide I	1651 (vs)	1651 (vs)	1654 (vs)
amide II	1551 (vs)	1560 (vs)	1560 (vs)
CH_2 scissoring	1465 (m)	1466 (m)	1475 (m)
CH_2 scissoring	1437 (m)	1438 (m)	1431 (m)
CH_2 wagging + amide III	1358 (m)	1354 (s)	1354 (vs)

[a] Very strong (vs), strong (s), medium (m), weak (w), and shoulder (sh).

these three spectra confirms (i) the dendrimer as an essential component of the composite nanoparticles and (ii) the dendrimer molecule was not removed after washings of the precipitate.

The bands at 3272 and 3068 cm^{-1} correspond to the amide A and B (NH stretching vibration modes), respectively. An observation of the spectra shows a slight shift of the amide A and B stretching frequencies to higher regions (to 3279 and 3080 cm^{-1}) after the adsorption on the metal particles. The characteristic bands assigned to amides I, II, and III are at 1651, 1551, and 1248 cm^{-1}, respectively. While the band position of amide I seems to be invariant, the amide II and III bands, respectively, shift slightly to higher (to 1560 cm^{-1}) and lower regions (to 1234 cm^{-1}) with respect to the adsorbed situation. The methylene groups show absorption bands due to the antisymmetric and symmetric stretching vibration modes at 2943 and 2830 cm^{-1} independent of the adsorption. The CH_2 scissoring and wagging modes at 1465, 1437, and 1358 cm^{-1} are slightly different among the three cases. All of these frequency changes indicate the conformational change of the G4 PAMAM dendrimer after the adsorption on the metal particles, indicating the interaction between particle and dendrimers.

The signals of the XPS spectrum in Figure 6 indicate the presence of Au, N, C, and O in the synthesized composite gold particles. The binding energies of these atoms were calculated on the basis of the binding energy (284.6 eV) of carbon. A high-resolution scan over the range 80−92 eV, which is shown as an insert in Figure 6, reveals a doublet of an Au($4f_{7/2}$) peak at around 83 eV and an Au($4f_{5/2}$) peak at around 86 eV. Another significant fact is that a shoulder on each peak was observed in the high-resolution spectrum. The peak positions, line shapes, and peak-to-peak distances are standard measures of the metal oxidation states.[30] The deconvolution of these peaks shows that each 4f peak consists of a pair with different intensities. The $4f_{7/2}$ peak at around 83 eV is split into a pair located at 83.3 and 82.4 eV, whereas the $4f_{5/2}$ peak at around 86 eV consists of a pair located at 86.8 and 86.1 eV. Thus, the data obtained from the XPS signal of the gold reveal two doublets of binding energies: 82.4 with 86.1 and 83.3 with 86.8 eV. The first doublet is located in the lower region with a binding energy separation of 3.7 eV, corresponding to the presence of the Au^0 state. This separation is exactly the same as the standard separation of the Au^0 doublet ($4f_{7/2}$ and $4f_{5/2}$).[5] The second pair with lower separation (3.5 eV) of the binding energy located in a higher region in comparison with the Au^0 indicates the existence of Au^{III} ions.[30] The existence of Au^{III} ions may be due to insufficient covering of the particle surfaces, which results in the formation of Au_2O_3 during washing, drying, and sampling of the composite materials since all the procedures were done in atmospheric conditions.

The nitrogen (N(1s)) and oxygen (O(1s)) regions exhibit peaks at 399.2 and 531.5 eV, respectively. The N(1s) and O(1s) core levels show a shift of about 1 and 1.5 eV, respectively, to the higher binding energy from the position expected for the unperturbed elements.[31] These shifts of the binding energies support the theory that the nitrogen and oxygen are components of organic amino and carbonyl (>C═O) groups, respectively.[31] Such oxidation states of N and O are expected for the dendrimer molecules.

The FT-IR and XPS analytical results described above indicate that (i) metal and dendrimer are essential

(29) (a) Lin-Vien, D.; Colthup, N. B.; Fateley, W. G.; Grasselli, J. G. *Infrared and Raman Characteristic Frequencies of Organic Molecules*; Academic Press: San Diago, 1991; Vol. 116; p 661. (b) Zeng, F.; Zimmerman, S. C. *Chem. Rev.* **1997**, *97*, 1681. (C) Zhao, M.; Tokuhisa, H.; Crooks, R. C. *Angew. Chem., Int. Ed.* **1997**, *36*, 2596.

(30) Pireaux, J. J.; Liehr, M.; Thiry, P. A.; Delrue, J. P.; Caudano, R. *Surf. Sci.* **1984**, *141*, 221.

(31) Barr, T. L. In *Modern ESCA, The Principles and Practice of X-ray Photoelectron Spectroscopy*; CRC Press: Boca Raton, FL, 1994; pp 224, 246.

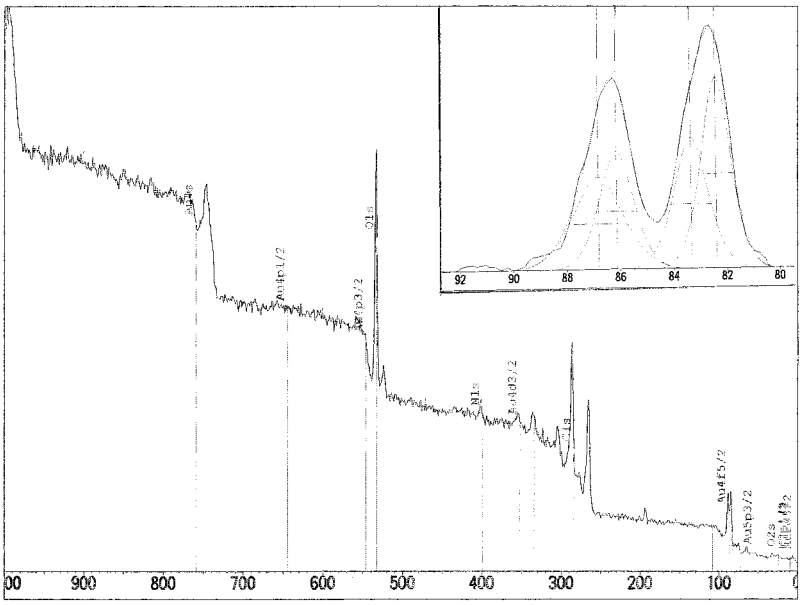

Figure 6. XPS spectra of the dry precipitate of the G4 PAMAM-stabilized gold nanoparticles: (a) Large scan and (b) high-resolution scan with deconvolution curves of the Au(4f) core level binding energy.

components of the composite materials and (ii) a strong interaction between metal particles and dendrimer molecules exists.

Conclusion

We have synthesized water-soluble G4 PAMAM dendrimer-passivated silver and gold nanoparticles with various ratios of metal ion to terminal amino groups of the G4 PAMAM dendrimer. UV−visible spectroscopic studies revealed the formation of nanoparticles and the lower energy plasmon absorption for the larger particle was seen. The TEM images confirm the size of the particles in the "quantum dot" range. The particle sizes depend on (i) the properties of the metal and (ii) the M:D ratio. The G4 PAMAM dendrimer-protected silver particles are substantially larger than the composite gold particles. This size difference may be due to the slower rate of reduction of silver ions to metallic silver and higher reactivity of silver Ag^0. The TEM image also indicates the formation of a monolayer of the dendrimer-protected nanoparticles onto the hydrophobic surfaces. Moreover, the particle size analysis by TEM supports the conclusion that the most active part of the dendrimer in nanoparticle stabilization is the terminal amino groups. FT-IR and XPS analyses indicate that the metal particles are encapsulated by the G4 PAMAM dendrimer. We believe that dendrimer-stabilized nanoparticles will find a unique position in many technological applications such as chemical sensor, membrane chemistry, selective electrochemical reactions, and catalysis due to their capacity for high functionality and molecular-sized channels.[29c,32]

CM000416B

(32) Bilewicz, R.; Majda, M. *J. Am. Chem. Soc.* **1991**, *113*, 5464.